

NASA Technical Memorandum 101443

# Strength of Hot Isostatically Pressed and Sintered Reaction Bonded Silicon Nitrides Containing $Y_2O_3$

William A. Sanders and Diane M. Mieskowski  
*Lewis Research Center*  
*Cleveland, Ohio*

(NASA-TM-101443) STRENGTH OF HOT  
ISOSTATICALLY PRESSED AND SINTERED REACTION  
BONDED SILICON NITRIDES CONTAINING  $Y_2O_3$   
(NASA) 10 p CSCL 11B

N89-15257

Unclas  
G3/27 0187912

January 1989

**NASA**

STRENGTH OF HOT ISOSTATICALLY PRESSED AND SINTERED REACTION  
BONDED SILICON NITRIDES CONTAINING  $Y_2O_3$

William A. Sanders and Diane M. Mieskowski  
National Aeronautics and Space Administration  
Lewis Research Center  
Cleveland, Ohio 44135

SUMMARY

The hot isostatic pressing of reaction bonded  $Si_3N_4$  containing  $Y_2O_3$  produced specimens with greater room temperature strengths than those by high pressure nitrogen sintering of the same material. Average room temperature bend strengths for hot isostatically pressed reaction bonded silicon nitride and high pressure nitrogen sintered reaction bonded silicon nitride were 767 and 670 MPa respectively. Values of 472 and 495 MPa were observed at 1370 °C. For specimens of similar but lower  $Y_2O_3$  content produced from  $Si_3N_4$  powder using the same high pressure nitrogen sintering conditions, the room temperature strength was 664 MPa and the 1370 °C strength was 402 MPa. The greater strengths of the reaction bonded silicon nitride materials in comparison to the sintered silicon nitride powder material are attributed to the combined effect of processing method and higher  $Y_2O_3$  content.

INTRODUCTION

In recent years,  $Si_3N_4$  and other Si-based ceramics have been studied as potential replacements for superalloys in high temperature environments. Their superior strengths make them likely candidates; however, they do not match the superalloys in reliability and fracture toughness. One approach to remedy these deficiencies in  $Si_3N_4$  has emphasized material strength improvement by the reduction of critical flaws in the  $Si_3N_4$  microstructures. The focus of the present study has been on flaw reduction in dense  $Si_3N_4$  through heat and pressure treatment of porous reaction-bonded  $Si_3N_4$ . Experiments involved the post-nitridation densification of reaction bonded  $Si_3N_4$  containing  $Y_2O_3$  by either hot isostatic pressing (HIP) or high pressure  $N_2$  (HPN) sintering. Processing effectiveness was evaluated by bend strength tests at room temperature and at 1370 °C.

Reaction bonded  $Si_3N_4$  is a desirable starting material because it can be up to 85 percent dense and therefore easily machined to near net-shape. The addition of a sintering aid, such as  $Y_2O_3$ , and an extra heat treatment are necessary to densify the material fully and to increase its strength to desired levels. This approach has been investigated by other researchers (refs. 1 to 9). A summary of their results follows. Giachello and Popper (ref. 1) and Mangels and Tennenhouse (refs. 2 to 4) conducted similar studies and were the first to report on the post sintering of RBSN containing  $Y_2O_3$ . In both projects the  $Y_2O_3$  was added to the Si powder prior to nitridation to obtain a final level of 8 wt %. (This level of  $Y_2O_3$  was chosen as the optimum level for both densification and high temperature strength retention.) Giachello and Popper used a sintering temperature of 1800 °C and  $N_2$  at atmospheric pressure. Mangels and Tennenhouse sintered at 1825 to 1925 °C and 2.07 MPa  $N_2$ .

Further work by Govila, Mangels, and Baer (ref. 8) involved a sintering temperature of 1975 °C, a pressure of 10 MPa N<sub>2</sub>, and a 2-stage sintering cycle. Other work on RBSN with Y<sub>2</sub>O<sub>3</sub> was performed by Pompe, Hermansson, and Carlsson (ref. 5) and by Falk, Pompe, and Dunlop (refs. 7 and 9). This differed from the preceding work in that Si<sub>3</sub>N<sub>4</sub> was mixed with Si and Y<sub>2</sub>O<sub>3</sub> prior to nitridation for the purpose of minimizing shrinkage. They reported 98 percent theoretical density and 11 to 12 percent total shrinkage for specimens sintered at 1870 °C and 1 atm N<sub>2</sub>.

The present study was based on RBSN to which Y<sub>2</sub>O<sub>3</sub> had been added prior to nitridation. Specimens were separated into two groups, one which was post-sintered at 2140 °C under 5.0 MPa N<sub>2</sub> and a second which was hot isostatically pressed at 1900 to 2050 °C under 138 MPa Ar. Strength averages were compared by statistical analysis using Student's t-test. Additional analysis included SEM for characterization of the general microstructure and critical flaws and TEM for characterization of the grain boundary phase.

### EXPERIMENTAL PROCEDURE

Fine powder was prepared by milling as-received minus 325 mesh (44 μm) silicon powder with 13.0 wt % Y<sub>2</sub>O<sub>3</sub> in a steel attrition mill. This level of Y<sub>2</sub>O<sub>3</sub> was calculated to yield 8.0 wt % Y<sub>2</sub>O<sub>3</sub> in Si<sub>3</sub>N<sub>4</sub> after nitridation and post-sintering Si loss. A powder batch weighing 300 g was mixed with 1.25 liters normal heptane and milled in air for 7 h. The milling media consisted of 3.2 mm diameter stainless steel balls with a media to powder weight ratio of 40:1. The resultant slurry was separated from the ball charge and air-dried to produce a friable powder cake. This was later passed through a 70 mesh (212 μm) sieve to facilitate preparation of test bars. Chemical analysis and specific surface area data are given in Table 1.

Test bars were made from the milled powder by cold compacting 1.6 g of powder containing no binder in a two-way-action tungsten carbide lined steel die at a pressure of 70 MPa. These bars were subsequently cold isostatically pressed at 350 MPa to green dimensions of 3.60 by 0.75 by 0.39 cm. Average green density was 62 percent of the calculated theoretical value of 2.50 g/cc for 87 wt % Si - 13 wt % Y<sub>2</sub>O<sub>3</sub>.

Weighed and measured test bars were placed on RBSN setters in groups varying from 12 to 23 bars. These in turn rested on high purity alumina trays which were placed in furnaces composed of high purity alumina tubes and external silicon carbide heating elements. After the furnace tubes were sealed and leak-checked, a flow of high purity He of 500 ml/min was established and the furnaces were purged for 2 h. The temperature was then increased linearly over a 4 h period to 1150 °C. The bars were sintered at 1150 °C for 4 h and allowed to cool to ambient temperature. At the completion of the sintering cycle, the He flow was stopped and an N<sub>2</sub> - 4 vol % H<sub>2</sub> flow of 10 ml/min was established. Both gases were purified to remove oxygen prior to introduction into the furnace. Exit gas from the nitriding furnace was passed through an oil filled bubbler which produced a back pressure of 0.023 MPa. Specimens were then nitrided following a cycle developed by Mangels and Williams (ref. 10). This schedule was of 140 h duration and had a maximum temperature of 1400 °C. The average specimen density after nitridation was 73 percent of the calculated theoretical value of 3.28 g/cc for 92 wt % Si<sub>3</sub>N<sub>4</sub> - 8 wt % Y<sub>2</sub>O<sub>3</sub>.

The test specimens were then divided into 2 groups of 45 for hot isostatic pressing and HPN sintering. Test bars receiving an HPN sinter were heated 15 at a time in a tungsten cup with a loose-fitting tungsten lid inside a water cooled double-wall furnace. The bars were separated from one another and from contact with the tungsten cup by BN discs. The loaded tungsten cup was placed on a tungsten pedestal with the axis of the pedestal centered in a 10.2 cm diameter tungsten mesh heater. Surrounding the heater were concentric W and Mo radiation shields. The sintering temperature (2140 °C) was monitored and controlled with W-5Re/W-26 Re thermocouples. Sintering time was 2 h in a static N<sub>2</sub> pressure of 5.0 MPa. Heating from R.T. to 2140 °C was at an approximately linear rate and accomplished in 45 min. Nitrogen pressure rise was also approximately linear, increasing from 0.7 MPa at the start of heating to 5.0 MPa within 60 min.

Those specimens subjected to HIP were clad in preformed Ta cans (0.05 cm thick) which had been coated with BN to prevent sticking. Prior to the final electron beam closure weld on the cans, specimens and cans were baked out in vacuum at 1000 °C for 2 h. Leak testing consisted of placement of the sealed cans under 6.9 MPa He pressure followed by immersion in alcohol and observation for bubbles. The Ta cans were then collapsed by cold isostatic pressing (414 MPa) to minimize deformation during HIP and rechecked for leaks. Canned specimens were placed in a graphite furnace housed within the HIP unit which had a 15 cm diameter by 15 cm long hot zone with a temperature uniformity of %10° at 2000 °C. The heat shield surrounding the hot zone was in the form of an inverted can and was fabricated from graphite and graphite wool. Specimens were then heated for 2 h at 1900 °C under 138 MPa Ar. Temperature was monitored with W-5Re/W-26 Re thermocouples having high purity BN for insulation. The Ta cans were removed from the specimens after HIP by oxidizing them in air at 1000 °C for 3 h. Of the original 45 test bars, 33 were lost due to breakage, related to nonuniform Ta can deformation.

Test specimens were prepared for strength testing by longitudinally grinding the major faces of the test bars with a 400 grit diamond wheel and beveling the long edges 0.12 mm. The final test bar cross section was 0.28 by 0.56 cm. Density measurements on machined test bars showed that 100 percent of theoretical density was attained by both HPN sintering and for HIP. Four point flexural strength tests were conducted at RT and 1370 °F. Steel fixtures having inner and outer spans of 9.53 and 19.05 mm, respectively, were used for room temperature tests. Elevated temperature tests were conducted using SiC fixtures with the same spans in an SiC muffle furnace mounted on a universal testing machine. All tests were conducted in air at a crosshead speed of 0.5 mm/min.

Additional analysis included chemical analysis of specimens after final heat treatment, SEM of fracture surfaces, and TEM examination of intergranular character.

## RESULTS AND DISCUSSION

In this section, strength and microstructural data will be compared for HPN sintered RBSN and HIP'd RBSN. This data will also be compared to previously reported data on NASA composition 6Y, a sintered Si<sub>3</sub>N<sub>4</sub> containing 6.2 wt % Y<sub>2</sub>O<sub>3</sub> and 0.13 wt % Fe which was HPN sintered under the same conditions (ref. 11). (Batches 15 and 16 reported in reference 11 are referred to in this report as NASA 6Y baseline.)

Table II shows a comparison of sintering results for HPN sintered RBSN with  $Y_2O_3$  and NASA composition 6Y baseline. Weight loss comparison with HIP'd RBSN was not feasible since this material had been canned in Ta. As expected, lower shrinkage and weight loss was obtained for RBSN bars in comparison to pressed  $Si_3N_4$  powder bars. The density difference is likely due to the higher  $Y_2O_3$  and Fe levels in the RBSN based material since both materials were essentially pore-free.

A summary of strength data for room temperature and 1370 °C is shown in Table III. Statistical analysis consisted of F-tests (comparisons of variances) and Student's t-tests (comparisons of means) at the 95 and 99 percent significance levels. All variances were found to be equal indicating that basic processing steps produced the same effects for all specimens. The t-tests indicated that: (1) the room temperature strength of HIP'd RBSN was greater than that of either HPN sintered RBSN or NASA 6Y at the 95 percent significance level; (2) HPN sintered RBSN and NASA 6Y showed equal strength; (3) the 1370 °C strength of HIP 'd and HPN sintered RBSN were equal; and (4) the 1370 °C strengths of both HIP'd and HPN sintered RBSN were greater than that of HPN sintered NASA composition 6Y baseline at the 99 percent significance level.

Neither SEM fractography nor microstructural analysis could account for the differences in strength. Critical flaws for all three materials were similar in size and diversity of shapes. Grain sizes and morphologies were similar. Likewise, TEM showed noncrystalline grain boundary phase for all of these materials. Representative micrographs showing a typical subsurface pore fracture origin obtained by SEM and the amorphous grain boundary phase obtained by TEM are shown figures 1 and 2 respectively.

The relative strengths of the materials studied are attributed to several different factors. These are described below in the same order as the relevant statistical statements.

1. The greater room temperature strength of HIP'd RBSN-base material over HPN sintered RBSN and NASA 6Y baseline is believed to result from the healing effects of HIP pressure on very fine cracks associated with the observed critical flaws.

2. The similar 1370 °C strengths of the RBSN-base materials are due to softening of their grain boundary phases which are identical in composition and phase.

3. The greater 1370 °C strength of the RBSN-base material over NASA 6Y baseline is likely due to a higher  $Y_2O_3$  content and more refractory grain boundary phase in the RBSN and also to the effect of HIP pressure on flaw severity.

Recent work by Sanders and Baaklini (ref. 11) show improvements in the strength of NASA 6Y with improvements in powder processing techniques. Similar benefits would be expected for RBSN materials.

#### CONCLUDING REMARKS

In this study, the RBSN route to a fully dense  $Si_3N_4$  material by hot isostatic pressing or high pressure nitrogen sintering has been demonstrated.

The fully dense RBSN-base materials were stronger than a sintered  $\text{Si}_3\text{N}_4$  material of similar composition. When employing high pressure nitrogen sintering, the RBSN-base material suffers less weight loss and shrinkage than the  $\text{Si}_3\text{N}_4$  powder-base material. These are beneficial attributes when considering component shapes for high temperature applications.

#### REFERENCES

1. A. Giachello and P. Popper, "Post-Sintering of Reaction-Bonded Silicon Nitride," pp. 620-31 in *Energy and Ceramics* (ed. by P. Vincenzini), Elsevier Scientific Publishing Co., New York, NY, 1980.
2. J.A. Mangels and G.V. Tennenhouse, "Densification of Reaction-Bonded Silicon Nitride," *Bull. Am. Cer. Soc.*, 59 (12), pp. 1216-18, 1222 (1980).
3. J.A. Mangels, "Sintered Reaction-Bonded Silicon Nitride," pp. 589-603 in *Proceedings of the 5th Annual Conference on Composites and Advanced Ceramic Materials*, American Ceramic Society, Columbus, OH 1981.
4. J.A. Mangels and G.J. Tennenhouse, "Sintering Behavior and Microstructural Development of Yttrium-Doped Reaction-Bonded Silicon Nitride," *Bull. Am. Cer. Soc.*, 60 (12), pp. 1306-10 (1981).
5. R. Pompe, L. Hermansson, and R. Carlsson, "Fabrication of Low-Shrinkage Silicon Nitride by Pressureless Sintering," pp. 65-74 in *Engineering with Ceramics* (ed. by R.W. Davidge), British Ceramic Society, Stoke-on-Trent, England, 1982.
6. J.A. Mangels, "Sintering of Reaction Bonded Silicon Nitride," pp. 231-6 in *Progress in Nitrogen Ceramics* (ed. by F.L. Riley), Martineus Nijhoff Publishers, Boston, Mass. 1983.
7. L.K.L. Falk, R. Pompe, and G.L. Dunlop, "Development of Microstructure during Nitridation and Sintering of Si: $\text{Si}_3\text{N}_4$  Powder Compacts," pp. 293-8 in *Science of Ceramics* (ed. by P. Vincenzini), Research Institute for Ceramics Technology, Faenza, Italy, 1983.
8. R.K. Govila, J.A. Mangels, and J.R. Baer, "Fracture of Yttria-Doped Sintered Reaction-Bonded Silicon Nitride," *J. Am. Cer. Soc.*, 68 (7), pp. 413-18 (1985).
9. L.K.L. Falk, R. Pompe, and G.L. Dunlop, "Development of Microstructure during the Fabrication of  $\text{Si}_3\text{N}_4$  by Nitridation and Pressureless Sintering of Si: $\text{Si}_3\text{N}_4$  Compacts," *J. Mat. Sci.*, 20 (10), pp. 3345-56 (1985).
10. J.A. Mangels and R.M. Williams, "Development of Moldable, High Density Reaction Bonded  $\text{Si}_3\text{N}_4$ ," Third Quarterly Report, Progress Report No. 9, Ford Motor Co., Dearborn, Mich., February, 1979. (NASA Contract DEN 3-20).
11. W.A. Sanders and G.Y. Baaklini, "Correlation of Processing and Sintering Variables with the Strength and Radiography of Silicon Nitride," NASA TM 87251 February, 1986.

TABLE I. - CHARACTERIZATION OF MILLED, NITRIDED, AND SINTERED MATERIAL

Material	Major components <sup>a</sup>			Chemical analysis	
	Si, wt %	Si <sub>3</sub> N <sub>4</sub> , wt %	Y <sub>2</sub> O <sub>3</sub> , wt %	wt%	ppm
Milled powder <sup>b</sup>	87	----	13	0.1Al, 1.0C, 1.7Fe, 6.60, 0.4Sn	50B, 0.2Ca, 640Cr, 720Mn, 240Ti, <0.1Zr
Nitrided RBSN	--	89.3	7.1	0.2C, 1.9Fe, 2.90 5.6Y	990Al, 200Ca, <0.01Co, 450Cr, <0.02Cu, <0.005Mg, 100Mn, <0.05Mo, <0.05Ni, 160Ti, <0.005V, <0.003Zn
HPN <sub>2</sub> SRBSN	--	89.1	7.1	0.05C, 1.9Fe, 2.80, 5.7Y	950Al, 200Ca, <0.01Co, 470Cr, <0.02Cu, <0.005Mg, 310Mn, <0.05Mo, <0.05Ni, 170Ti, <0.005V, <0.003Zn
HIP'D SRBSN	--	89.4	7.1	0.1C, 1.9 Fe, 3.10, 5.6Y	980Al, 190Ca, <0.01Co, 450Cr, <0.02Cu, <0.005Mg 360Mn <0.05 Mo, <0.05Ni 160Ti, <0.005V, <0.003Zn

<sup>a</sup>As added for milled powder; calculated for other materials based on chemical analysis.

<sup>b</sup>Specific surface area from 3-point BET, 14.2 m<sup>2</sup>/g.

TABLE II. - SINTERED RESULTS FOR RBSN AND Si<sub>3</sub>N<sub>4</sub> POWDER COMPACTS  
SINTERED AT 2140 °C FOR 2 HR UNDER 5 MPa NITROGEN

Material	Sintering result		
	Weight loss, percent	Width shrinkage, percent	Machined density, g/cm <sup>3</sup>
RBSN	1.52	10.4	3.29
Si <sub>3</sub> N <sub>4</sub> powder <sup>a</sup>	4.77	17.0	3.22

<sup>a</sup>For NASA composition 6Y, ref. 11.

TABLE III. - STRENGTH STATISTICS FOR HIGH PRESSURE NITROGEN SINTERED RBSN WITH Y<sub>2</sub>O<sub>3</sub>, HIP'D RBSN WITH Y<sub>2</sub>O<sub>3</sub>, AND HIGH PRESSURE NITROGEN SINTERED NASA COMPOSITION 6Y

Material	Four-point flexural strength			
	Temperature, °C	Number of bars	Average strength, MPa	Standard deviation, MPa
HPN <sub>2</sub> Sint. RBSN	RT	14	670	77
	1370	15	495	50
HIP'D RBSN	RT	5	767	69
	1370	14	472	55
NASA 6Y (ref. 11)	RT	19	664	85
	1370	20	402	52

ORIGINAL PAGE IS  
OF POOR QUALITY

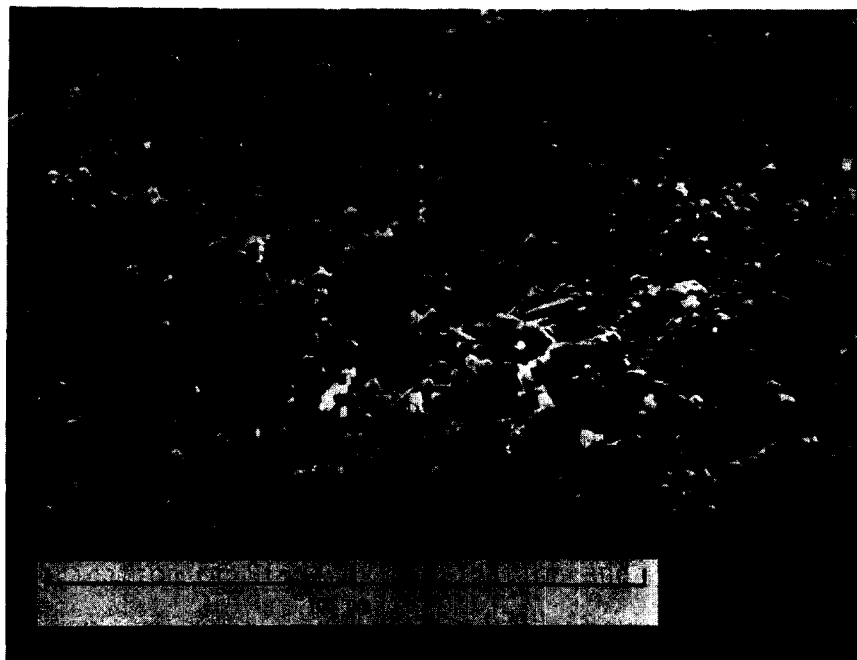


FIGURE 1. - SCANNING ELECTRON MICROGRAPHS OF ROOM TEMPERATURE FRACTURE ORIGIN IN HIGH PRESSURE NITROGEN SINTERED RBSN.



ORIGINAL PAGE IS  
OF POOR QUALITY



(A) BRIGHT FIELD MICROSTRUCTURE (GRAIN BOUNDARY PHASE APPEARS DARK).



(B) DARK FIELD MICROSTRUCTURE (GRAIN BOUNDARY PHASE APPEARS LIGHT).

FIGURE 2. - TRANSMISSION ELECTRON MICROGRAPHS DELINEATING AMORPHOUS GRAIN BOUNDARY PHASE FOR HIGH PRESSURE NITROGEN SINTERED RBSN.

1. Report No. NASA TM-101443		2. Government Accession No.		3. Recipient's Catalog No.	
4. Title and Subtitle Strength of Hot Isostatically Pressed and Sintered Reaction Bonded Silicon Nitrides Containing $Y_2O_3$				5. Report Date January 1989	
				6. Performing Organization Code	
7. Author(s) William A. Sanders and Diane M. Mieskowski				8. Performing Organization Report No. E-4429	
				10. Work Unit No. 505-63-01	
9. Performing Organization Name and Address National Aeronautics and Space Administration Lewis Research Center Cleveland, Ohio 44135-3191				11. Contract or Grant No.	
				13. Type of Report and Period Covered Technical Memorandum	
12. Sponsoring Agency Name and Address National Aeronautics and Space Administration Washington, D.C. 20546-0001				14. Sponsoring Agency Code	
15. Supplementary Notes					
16. Abstract <p>The hot isostatic pressing of reaction bonded <math>Si_3N_4</math> containing <math>Y_2O_3</math> produced specimens with greater room temperature strengths than those by high pressure nitrogen sintering of the same material. Average room temperature bend strengths for hot isostatically pressed reaction bonded silicon nitride and high pressure nitrogen sintered reaction bonded silicon nitride were 767 and 670 MPa respectively. Values of 472 and 495 MPa were observed at 1370 °C. For specimens of similar but lower <math>Y_2O_3</math> content produced from <math>Si_3N_4</math> powder using the same high pressure nitrogen sintering conditions, the room temperature strength was 664 MPa and the 1370 °C strength was 402 MPa. The greater strengths of the reaction bonded silicon nitride materials in comparison to the sintered silicon nitride powder material are attributed to the combined effect of processing method and higher <math>Y_2O_3</math> content.</p>					
17. Key Words (Suggested by Author(s)) Hot isostatic pressing High pressure nitrogen sintering Sintered reaction bonded silicon nitride Flexural strength			18. Distribution Statement Unclassified - Unlimited Subject Category 27		
19. Security Classif. (of this report) Unclassified		20. Security Classif. (of this page) Unclassified		21. No of pages 10	22. Price* A02